Spatial Gain Measurements in a Chemical Oxygen Iodine Laser (COIL)

R. F. Tate, B. S. Hunt, C. A. Helms, K. A. Truesdell, and G. D. Hager

Abstract— **The spatial distribution of small signal gain has been investigated on the RADICL device, a supersonic chemical oxygen-iodine laser (COIL). A frequency-stabilized, narrow linewidth diode laser system operating on the $F = 3 \rightarrow F = 4$ hyperfine levels of the $(^2P_{1/2})$ to $(^2P_{3/2})$ spin-orbit transition in atomic iodine was used as a small signal probe. A peak gain of 1.2%/cm was measured along the horizontal centerline of the single-slit, supersonic nozzle, which is about two times greater than measurements made on ReCOIL by Hager *et al.* and compares favorably with measurements made on the RotoCOIL device by Keating *et al.* Gain distribution was investigated under three I_2 flow conditions. Scans across the supersonic expansion indicate a gradient in gain distribution due to higher gas temperatures along the walls and mixing phenomena.**

I. Background

THE chemical oxygen iodine laser (COIL) operates on the $I(^2P_{1/2}) \rightarrow I(^2P_{3/2})$ transition of atomic iodine and is pumped via energy transfer from the $a^1\Delta$ state of molecular oxygen. The generation of $O_2(^1\Delta)$ is governed by the following chemical reaction:

$$Cl_2 + 2O_2H^- \rightarrow O_2(^1\Delta) + H_2O_2 + 2Cl^-. \quad (1)$$

The oxygen gas flows into the laser cavity after the introduction of I_2 by sidewall injection, just upstream of the sonic throat. The dissociation of I_2 is a complex process involving energy pooling [3], but can be described globally according to (2)

$$nO_2(^1\Delta) + I_2 \rightarrow nO_2(^3\Sigma) + 2I + \Delta H(n), \quad (2)$$

where n represents the number of $O_2(^1\Delta)$ molecules required to dissociate one I_2 molecule, and $\Delta H(n)$ is the heat released as a function of n [1]. Energy transfer from $O_2(^1\Delta)$ to atomic iodine is rapid and results in spin-orbit excited iodine atoms as shown in (3).

$$I(^2P_{3/2}) + O_2(^1\Delta) \underset{k_r}{\overset{k_f}{\rightleftarrows}} I(^2P_{1/2}) + O_2(^3\Sigma). \quad (3)$$

Energy extraction via stimulated emission completes the COIL system description and can be written as

$$I(^2P_{1/2}) + h\nu \rightarrow I(^2P_{3/2}) + 2h\nu(1.315\,\mu m). \quad (4)$$

Manuscript received March 16, 1995.

The authors are with LIDB, Phillips Laboratory, 3550 Aberdeen Avenue, S.E., Kirtland Air Force Base, NM 87117–5776 USA.

IEEE Log Number 9413346.

II. Supersonic Nozzle

Fig. 1 depicts the nozzle assembly of the COIL. It is a single-slit, supersonic nozzle with a throat area of 0.9 × 25 cm. Molecular iodine in a helium carrier is transversely injected into the subsonic flow of oxygen via two rows of holes (0.016″ and 0.032″) along the 25-cm dimension of the nozzle plenum. The I_2 is $\geq$90% dissociated by the time the flow field reaches the throat under the flow conditions discussed here [4]. The flow field experiences a 2 : 1 expansion and reaches supersonic (Mach 2.4) velocity within the cavity.

Ideally, the iodine flow would fully penetrate the oxygen flow and the concentrations of oxygen and iodine would be uniform across the expansion. If the iodine flow does not fully penetrate the oxygen flow, an iodine poor region develops along the centerline of the expansion [5]. In addition, pitot tube measurements indicate that a subsonic boundary layer is present at the walls of the expansion, which reduces the concentration of I^* near the walls. Note that complete penetration of the iodine stream to the centerline of the core flow does not constitute homogenous distribution of iodine in the main flow.

III. Experimental

A frequency-stabilized, line-narrowed, single-mode diode laser system was used as a small signal probe to determine the gain distribution of the COIL. Fig. 2 depicts the diode laser system. This laser has been used to measure gain on a photolytic iodine laser and has been previously described [6]. Output of the laser is single mode, with an instrument-limited measured linewidth of $\leq$5 MHz full width half maximum (FWHM), and an average power of 1 mW. The laser is maintained at the wavelength of the 3–4 hyperfine transition in atomic iodine via a heated iodine absorption cell. The output beam is coupled into a single-mode fiber and is routed to the RADICL device.

The probe beam was passed through the gain medium of the COIL along the optical axis, transverse to the flow direction as shown in Fig. 3. The beam diameter was 2.5 mm and the gain length was 25 cm. A polarizer and bandpass filter were used to reduce the effects of spontaneous I^* and I_2 emission on the room temperature germanium detector. The probe beam was translated both along and across the expansion.

Fig. 4 shows the output of the detector with gain present. The initial voltage value is proportional to I_0, the initial intensity, and the increased voltage value is proportional to I, the amplified intensity. The decay in the gain signal is attributed to quenching of $[I^*]$ by water vapor and has also been observed in power measurements. The gain per unit

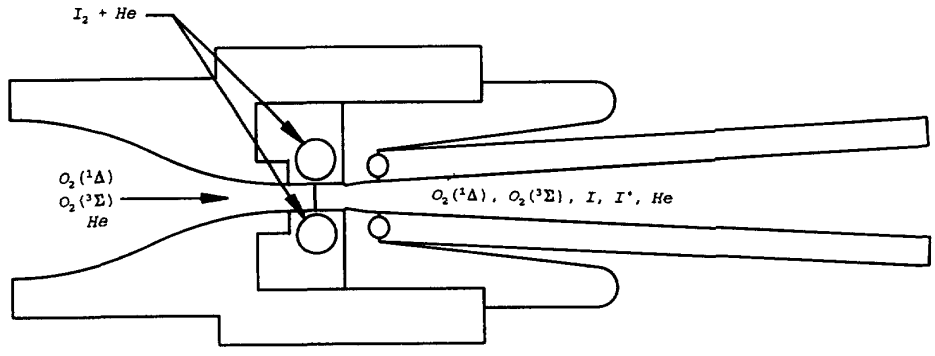

Fig. 1. COIL supersonic nozzle. The expansion ratio of 2:1 produced a MACH 2.4 flow in the cavity region.

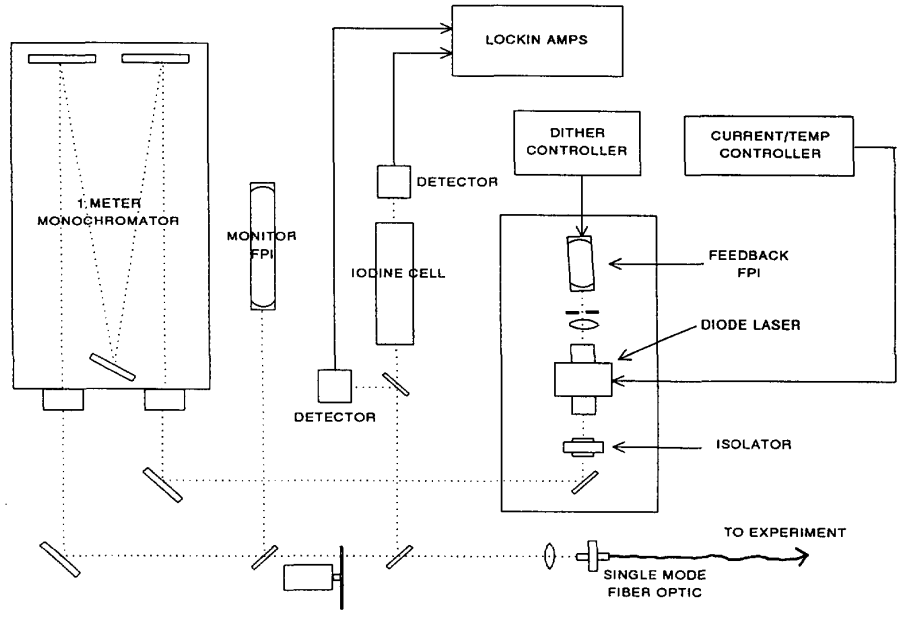

Fig. 2. Diode laser system.

length is easily calculated by

$$G(\%/\text{cm}) = \frac{\ln \dfrac{\text{I}}{\text{I}_0}}{25\,\text{cm}}\,100. \tag{5}$$

IV. Test Conditions

Three series of tests were conducted to investigate the effects on the gain distribution by changing flow conditions. In all three test series, the chlorine flow was maintained at 0.5 mole/s and the helium carrier for chlorine was maintained at 1.5 mole/s. A nominal I_2 flow rate of 0.007 mole/s was maintained for test series one in order to establish a baseline for the gain data.

In test series two, the I_2 flow rate was increased to 0.01 mole/s and the iodine carrier helium (secondary) was decreased to maintain constant jet penetration according to the formula:

$$\Pi = \frac{n_s}{n_p}\left(\frac{M_s T_s P_p}{M_p T_p P_s}\right)^{1/2} \tag{6}$$

where: n is the molar flow rate, M is the average molecular weight, T is the gas temperature, P is the pressure, and the subscripts "s" and "p" represent secondary and primary flow, respectively. In test series three, the helium carrier for I_2 was decreased, causing an underpenetrated condition. Table I lists all the flow rates for the three test series.

V. Results

Fig. 5 is a plot of the centerline gain distribution for the nominal and high I_2 flow cases. Error bars on the high I_2 data indicate the range of data collected over 7 shots and equals ±0.15%/cm. Vertical scans across the expansion were made in 0.5 cm increments, beginning at the centerline and going to the walls of the expansion. Figs. 6, 7, and 8 show the plots for the three cases investigated.

Data were collected along the centerline of the expansion and across the expansion at various positions. Probing was restricted by hardware to include an area bounded from 4 cm downstream from the throat to 15 cm downstream from the

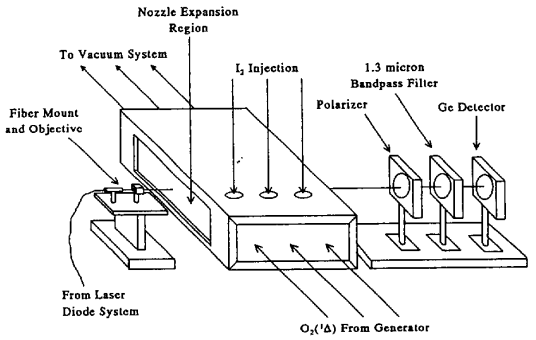

Fig. 3. Experimental approach.

TABLE I
TEST SERIES FLOW RATES

	Flows (mole/s)		
Gas	Nominal	High I_2	Underpenetrated
Cl_2	0.5	0.5	0.5
$He_{primary}$	1.5	1.5	1.5
I_2	0.007	0.01	0.007
$He_{secondary}$	0.65	0.58	0.29

Cl_2 Utilization = 0.85 Yield = 0.45 to .60

throat. Scans across the expansion were made at the highest centerline gain position, at the "typical" optical centerline (9 cm from throat), and at a position downstream from the optical centerline. Data were collected at a 10-Hz rate during the 3-s chlorine run times.

VI. DISCUSSION

A comparison of the two plots in Fig. 5 shows no appreciable change in centerline gain as the I_2 flow was increased. One possible explanation for this result can be drawn from (2). Increasing the I_2 flowrate would increase the heat released during dissociation, resulting in a decrease in $O_2(^1\Delta)$ and $I(^2P_{1/2})$ concentrations. The centerline gain data presented here, along with previous gain measurements on the ReCOIL and ROTOCOIL devices, can be compared with the results of a 1-dimensional, premixed model, shown in the Appendix. Table II lists relevant parameters and peak measured gain for all three devices and also shows the predicted gain calculated from list parameters, assuming uniform, premixed conditions.

Figs. 6 and 7 reveal little difference in the gain distribution across the expansion as a function of I_2 flow rate. The parabolic distribution of gain across the expansion indicates a gradient in flow composition. This is most likely due to a combination of mixing phenomena and boundary layer development along the walls. For the underpenetrated case depicted in Fig. 8, the bimodal gain distribution across the expansion shows an obvious reduction in $I(^2P_{1/2})$ concentration along the centerline of the flow.

The model assumes a cavity temperature of 150 K, an n of 5 [from (2)], an $O_2(^1\Delta)$ yield of 60 percent in the nozzle plenum, an 85-percent chlorine utilization for oxygen generation, and an I_2 dissociation of 95 percent. These values are somewhat arbitrary but do fall within bounds established

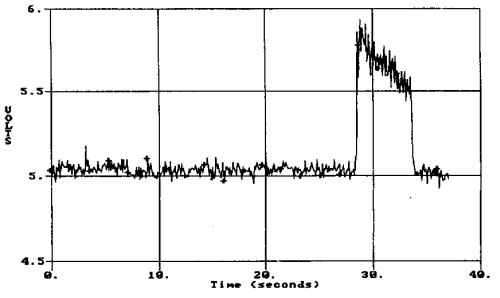

Fig. 4. Gain signal.

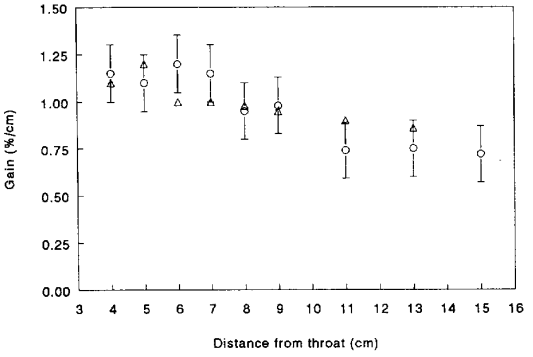

Fig. 5. Centerline gain distribution for the nominal I_2 case (Δ) and the high I_2 case (0). Error bars indicate the repeatability of the measurements.

by theoretical models and experimental data [1], [4], [7]. The model was intended to provide a first order prediction of single-point gain, not necessarily to fit all experimental data.

For the RADICL and ReCOIL data, there is good agreement between the measured and predicted values on each device, but there is nearly a factor-of-two difference between the gain measurements, primarily due to differences in cavity pressure, hardware, and flow conditions. Both devices employ a single-slit nozzle with similar dimensions, but ReCOIL used a Sparger generator, resulting in lower operating pressures and lower concentrations of oxygen and iodine in the cavity region [1].

A comparison of RADICL and RotoCOIL gain data reveals a difference in gain values of about a factor of two as well. Again, differences in hardware provide an explanation. Both devices use rotating disk generators, but RotoCOIL employed a multiple-slit nozzle bank with a 54-cm gain length in the cavity [7]. I* profile studies performed on the RotoCOIL device [8] revealed a wake and core structure in the gain distribution along the optical axis, an attribute of the multiple-slit nozzle bank. Therefore, the peak gain of 0.65%/cm on the RotoCOIL device is an average measurement made across alternating regions of high and very low gain [9]. This accounts for the approximate factor-of-two difference in peak gain values for the two COIL devices with similar flow conditions.

VII. SUMMARY

The small signal gain distribution in the cavity of a supersonic COIL (RADICL) has been investigated for three I_2 flow

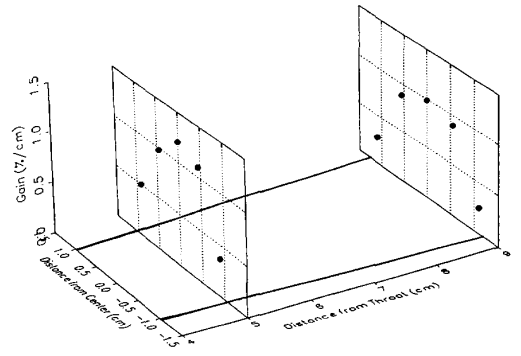

Fig. 6. Small signal gain measured across the expansion at two locations for the nominal I_2 case (see Table I).

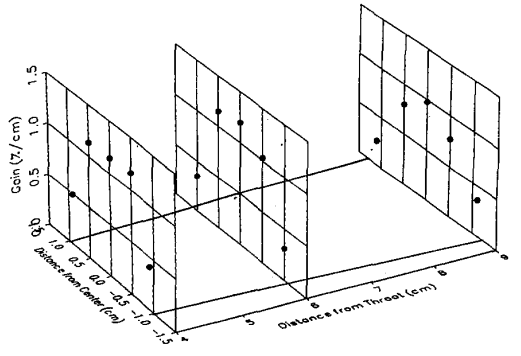

Fig. 7. Small signal gain measured across the expansion at three locations for the high I_2 case (see Table I).

conditions. Gain did not change as a function of increased I_2 flow (within the uncertainty of the measurement). A bimodal gain distribution was observed across the expansion when the I_2 flow did not fully penetrate the oxygen flow. This was expected based on the LIF data collected during the COIL nozzle development programs and theoretical calculations. [10] $I_2(b - X)$ emission has always shown a gap in the center for underpenetrated cases. Comparisons to previous gain measurements on the RotoCOIL device are favorable, and the factor-of-two difference between RADICL and ReCOIL gain measurements can be attributed to differences in hardware and flow conditions. Future efforts will concentrate on developing a two-dimensional temperature map of the COIL cavity via direct gain linewidth measurements.

APPENDIX

A simple theory can be developed to predict single point gain within the cavity of a COIL. This theory is based on the assumption that the iodine is dissociated upstream of the nozzle throat and is completely mixed with the oxygen. It is also assumed that the oxygen and atomic iodine are in equilibrium such that:

$$k_f[O_2(^1\Delta)][I] = k_r[O_2(^3\Sigma)][I^*]. \tag{7}$$

An equilibrium rate constant can be calculated thermodynamically in terms of degeneracies, exothermicity, and the

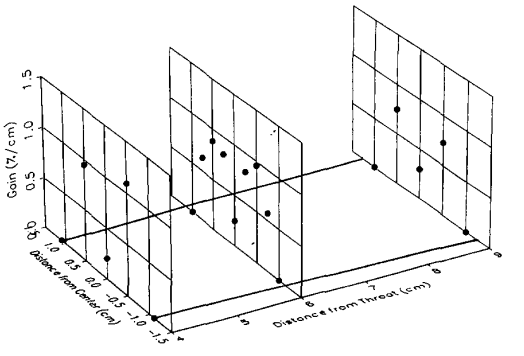

Fig. 8. Small signal gain measured across the expansion at three locations for the underpenetrated case (see Table I).

TABLE II
GAIN COMPARISON

Parameters	RADICL	ReCOIL	RotoCOIL	Units
Cl_2	0.5	0.1	1.55	moles/s
$He_{primary}$	1.5	0.3	4.56	moles/s
I_2	0.007	0.00143	0.022	moles/s
$He_{secondary}$	0.65	0.1	0.9	moles/s
I_2/O_2	1.5	1.68	1.67	percent
P_{plenum}	75	17.4	44.6	torr
P_{cavity}	5.8	2.38	3.9	torr
Measured Gain	1.2	0.6	0.65	percent/cm
Premixed Gain Prediction	1.25	0.58	1.0	percent/cm

temperature [1].

$$k_{eq}(T) = \frac{k_f}{k_r} = 0.75 \exp\left(\frac{402}{T}\right). \tag{8}$$

Combining (7) and (8) gives:

$$\frac{[I^*]}{[I]} = k_{eq}(T)\,\frac{[O_2(^1\Delta)]}{[O_2(^3\Sigma)]}. \tag{9}$$

Knowing

$$[I^*] + [I] = [I_{TOT}] \tag{10}$$

and

$$[O_2(^1\Delta)] + [O_2(^3\Sigma)] + [O_2(^1\Sigma)] = [O_{2TOT}] \tag{11}$$

and neglecting $O_2(^1\Sigma)]$ in (11), (9) can be solved for [I] and [I*]:

$$[I] = \frac{[I_{TOT}][1 - Y(n)]}{[1 - Y(n)] + k_{eq}(T)Y(n)} \tag{12}$$

$$[I^*] = \frac{[I_{TOT}]k_{eq}(T)Y(n)}{[1 - Y(n)] + k_{eq}(T)Y(n)}. \tag{13}$$

The quantity $Y(n)$ in (12) and (13) represents the local yield of $O_2(^1\Delta)$. It can be expressed in terms of the initial yield measured in the plenum minus the number n of $O_2(^1\Delta)$ used in the dissociation of I_2.

$$Y(n) = Yield_{plenum} - n\frac{N_{I_2}}{N_{O_2}}. \tag{14}$$

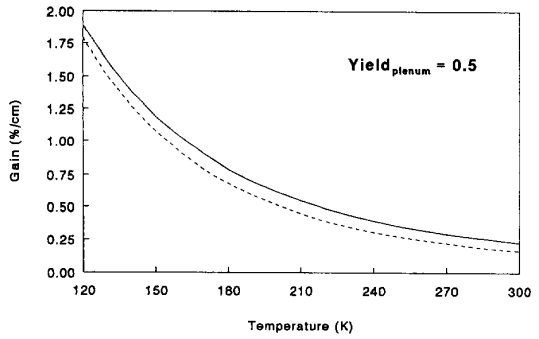

Fig. 9. Dependence of predicted SSG on temperature and for $n = 2$(——) $n = 10$(- - - -).

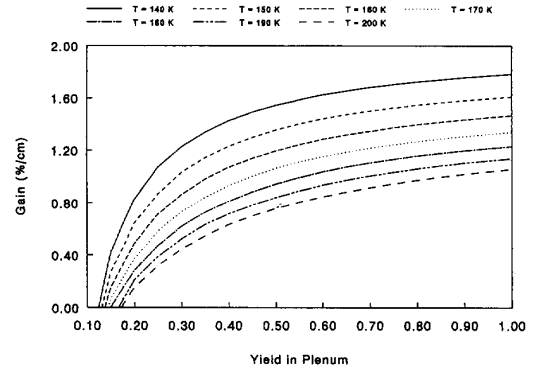

Fig. 10. Dependence of predicted SSG on temperature and plenum yield.

The small signal gain in an iodine laser can be expressed as:

$$g = \frac{7}{12}\frac{A\lambda^2}{8\pi} f(\nu)\left([\mathrm{I}^*] - \frac{1}{2}[\mathrm{I}]\right), \tag{15}$$

where A is the Einstein A coefficient, λ is the transition wavelength, and $f(\nu)$ is the lineshape function. Substituting (12) and (13) for [I] and [I*] in (15) yields:

$$g = \frac{7}{12}\frac{A\lambda^2}{8\pi} f(\nu)\frac{\mathrm{I}_{TOT}}{2}\frac{Y(n)[2k_{eq}(T)+1]-1}{Y(n)[k_{eq}(T)+1]+1}. \tag{16}$$

The transition lineshape in a COIL operating under nominal conditions is best described with a Voigt lineshape function: [6]

$$f(\nu)_v = f(\nu)_G \mathrm{Re}\{W(z)\}, \tag{17}$$

where the complex error function $W(z)$ can be evaluated with:

$$w(z) = \sum_{n=0}^{\infty} \frac{(iz)^n}{\Gamma\left(\frac{n}{2}+1\right)} \tag{18}$$

and $f(\nu)_G$ is the general expression for a Gaussian lineshape function. At line center $\nu = \nu_0$, and (16) can be reduced to:

$$f(\nu_0)_v = \frac{2}{\Delta\nu_D}\sqrt{\ln\frac{2}{\pi}}\,\mathrm{Re}\left\{W\left(\frac{\Delta\nu_L}{\Delta\nu_D}\sqrt{\ln 2}\right)\right\}, \tag{19}$$

where $\Delta\nu_D$ and $\Delta\nu_L$ are the Doppler and Lorentzian linewidths, respectively.

Equation (16) can be evaluated numerically to allow parametric studies of the small signal gain as a function of local temperature, yield, and n. Direct measurements of local temperature, yield, and n have not yet been attempted. However, theoretical bounds can be applied to each quantity to limit the parameter space. Figs. 9 and 10 illustrate the sensitivity of the small signal gain to the three bound parameters.

REFERENCES

[1] G. D. Hager, L. J. Watkins, R. K. Meyer, D. E. Johnson, L. J. Bean, and D. L. Loverro, "A supersonic chemical oxygen-iodine laser," US Air Force Weapons Lab., Kirtland AFB, NM, AFWL-TR-87-45, Jan. 1988.

[2] P. Keating, L. Hanko, and K. A. Truesdell, "RotoCOIL small signal gain experiments," *Laser Dig.*, WL-TR-89-46, US Air Force Weapons Laboratory, Kirtland AFB, NM, pp. 167–176, Jan 1990.

[3] R. F. Heidner, III, C. E. Gardner, G. I. Segal, and T. M. El Sayed, "Chain-reaction mechanism for I_2 dissociation on the $O_2(^1\Delta)$ I-atom laser," *J. Phys. Chem.*, vol. 87, no. 13, 1983.

[4] C. A. Helms, "Iodine dissocation in COILs," in *AIAA 25th Plasmadynamics and Lasers Conf.*, Colorado Springs, CO, June 20–23, 1994, Paper 94-2437.

[5] ——, Air Force Phillips Laboratory, Kirtland AFB, NM, private communication, Feb. 1994.

[6] B. S. Hunt, "Parametric studies on a short pulsed KrF pumped atomic iodine laser," M.S. thesis, Univ. of New Mexico, Albuquerque, NM, 1993, pp. 86–87.

[7] K. A. Truesdell, S. E. Lamberson, and G. D. Hager, "Phillips Laboratory COIL technology overview," presented at the 23rd AIAA Plasmadynamics and Lasers Conf., Nashville, TN, July 6–8, 1992.

[8] L. Hanko, K. A. Truesdell, and P. Keating, "$I(^2P_{1/2})$ concentration and profiles," *Laser Dig.*, WL-TR-89-46, US Air Force Weapons Lab., Kirtland AFB, NM, pp. 119–127, Jan. 1990.

[9] J. E. Scott, K. A. Truesdell, C. A. Helms, J. Shaw, and G. D. Hager, "Design considerations for the chemical ozygen-iodine laser," in *AIAA 25th Plasmadynamics and Lasers Conf.*, Colorado Springs, CO, June 20–23, 1994, Paper 94-2436.

[10] J. Hon, D. Plummer, P. Crowell, K. A. Truesdell, and G. D. Hager, "A heuristic view of COIL efficiency," in *AIAA 25th Plasmadynamics and Lasers Conf.*, Colorado Springs, CO, June 20–23, 1994, Paper 94-2422.

R. F. Tate, photograph and biography not available at the time of publication.

B. S. Hunt, photograph and biography not available at the time of publication.

C. A. Helms, photograph and biography not available at the time of publication.

K. A. Truesdell, photograph and biography not available at the time of publication.

G. D. Hager, photograph and biography not available at the time of publication.